THE STRUCTURE OF TURBULENT AIR FLOW OVER WAVY WALL. PART 1

Bandou, Toshiyuki
Department of Civil Engineering Hydraulics and Soil Mechanics, Kyushu University : Graduate student

Mitsuyasu, Hisashi
Reserch Institute for Applied Mechanics, Kyushu University : Professor

Marubayasi, Kenji
Reserch Institute for Applied Mechanics, Kyushu University : Technical assistant

Isibasi, Michiyosi
Reserch Institute for Applied Mechanics, Kyushu University : Technical assistant

https://doi.org/10.5109/6781055

出版情報：Reports of Research Institute for Applied Mechanics. 34 (103), pp.53-65, 1988-02. 九州大学応用力学研究所
バージョン：
権利関係：

Reports of Research Institute for Applied Mechanics
Vol. XXXIV, No. 103, 1988

THE STRUCTURE OF TURBULENT AIR FLOW OVER WAVY WALL. PART 1

By Toshiyuki BANDOU*, Hisashi MITSUYASU†, Kenji MARUBAYASI‡ and Michiyosi ISIBASI‡

Measurements of the pressure distribution along the solid wavy surface under the action of turbulent wind are presented for the sinusoidal wave and the Stokes wave, both of which have the same height-to-length ratio $H/L = 0.1$. The experiment covers the range of the Reynolds numbers U_0H/ν from 4,000 to 14,000, where U_0 is the maximum wind speed over the wavy surface, H the height of the waves and ν the coefficient of kinematic viscosity of the air.

Pressure measurements indicate that the pressure distribution along both wavy surfaces are described well by the first mode of the waves with the wave length equal to that of the wavy surfaces. Amplitudes of the first mode of the pressure profiles for both waves are nearly equal but the phase shifts relative to the waves are larger for the Stokes wave than for the sinusoidal wave. Thus the pressure drag coefficient of the Stokes waves is larger than that of the sinusoidal wave. An empirical relation between the Reynolds number and the pressure drag coefficient normarized by the maximum slope of wavy surfaces have been obtained, which can be applied to the Stokes waves as well as the sinusoidal waves with various steepness.

key words : turbulent flow over wavy surface, wind wave generation, wind-wave interaction, pressure drag coefficient, sheltering coefficient

1. Introduction

It is very important to investigate the flow structures over water waves to clarify the growth mechanism of wind-generated waves. Although quite many studies have been conducted on this problem, we are still not in the position to derive satisfactory answers due to the difficulties of the problem. One of the difficulties is due to the complexity of the phenomena itself, but another one is the experimental difficulties in the measurements of the flow structure over the

* Graduate student, Department of Civil Engineering Hydraulics and Soil Mechanics, Kyushu University
† Professor, Reserch Institute for Applied Mechanics, Kyushu University.
‡ Technical assistant, Reserch Institute for Applied Mechanics, Kyushu University.

moving water surface.

In order to reduce the experimental difficulties and to obtain the detailed data on the flow structure over the wavy surface, we are conducting, as a first step, the measurements of the flow structure over solid waves with various wave form. Although some differences are naturally expected between the flow structure over the solid waves and that over the moving water waves, the detailed studies on the flow structure over the solid waves under various conditions will present important informations. Several studies have been conducted along this line, typical of which are those by Motzfeld[1], Kendall[2], Zilker et al [3)4)] and Buckles et al[5]. However, since their experimental conditions are limitted, there still remain many problems to derive a satisfactory conclusion.

Our present study is mainly concerned with the pressure distributions along the wavy surfaces. In order to clarify the effect of the wave form on the pressure distributions, we used two waves; a sinusoidal wave and the Stokes wave, both of which have the same height-to-length ratio (wave steepness) $H/L = ak/\pi = 0.1$ and the wave length 20 cm, where a is the wave amplitude and k the wave number defined by $2\pi/L$. The previous data reported by Motzfeld[1] and Kendall[2] will be also used in the parameterization of the pressure drag coefficients.

2. Experiment

The experiment was carried out in a wind wave channel, 0.8 m high, 0.6 m wide and 14.6 m long. The test plate with wavy surface was installed horizontally in the wind wave channel as shown in Fig. 1.

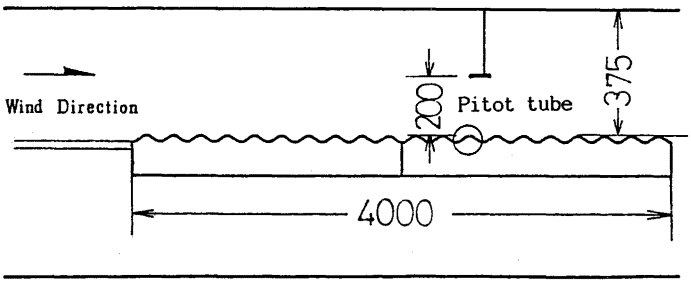

Figure 1 Schematic diagram of the test section: ○, measuring station. (Unit in mm)

In the present study, we used two types of waves with wave length of 20 cm, and height-to-length ratio (steepness) of $H/L = 0.1$.

The first one is a sinusoidal wave given by

$$\eta = a \cos kx \ , \quad k = 2\pi/L$$

The second one is a Stokes wave given by

$$\eta = \sum_{i=1}^{4} a_i \cos k_i x \ , \quad k_i = 2\pi/L_i$$

Table 1 shows the form parameters of these waves. The Stokes wave is slightly different from the forth order approximation of the waves due to an error in the production procedure. However, since the difference is small, this will not be serious to investigate the effect of higher harmonics of the waves on the pressure distributions along the wavy surface.

Twenty pressure holes were drilled on the solid waves as shown in Fig. 2. The short pipe having an inner diameter of 1.0 mm was inserted in each hole. The pressure holes are located from wind ward trough to leeward trough of the 13th wave from the leading edge of the waves. The horizontal separation distance of each pressure hole to the streamwise direction is 1.0 cm.

Each pressure hole was connected to the pressure transducer through a pressure-changeover equipment as schematically shown in Fig. 2. Another side

Table 1 The form parameters of the test waves: the blakets show the parameters of the forth order approximation of the Stokes wave.

Model	*Wave*	*H/L*	$(ak)_1$	$(ak)_2$	$(ak)_3$	$(ak)_4$
I	sine	0.1	0.314	0	0	0
II	Stokes	0.1	0.308	0.0779	0.0179	0.0053
			(0.304)	(0.0929)	(0.0315)	(0.0113)

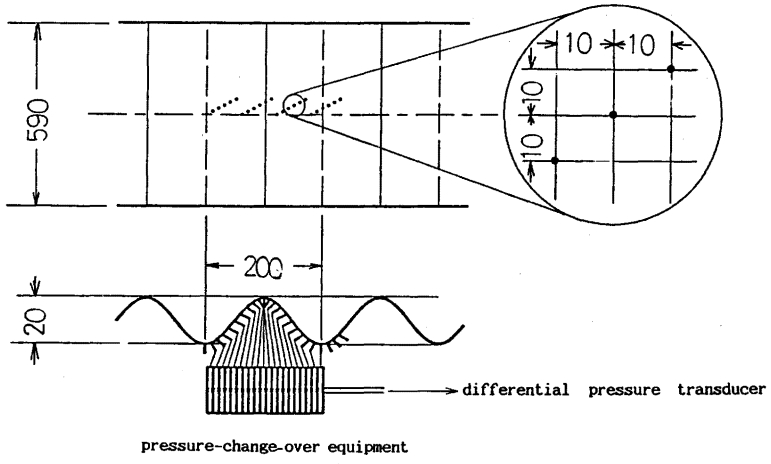

Figure 2 The configuration of the static pressure holes in the measuring station. (Unit in mm)

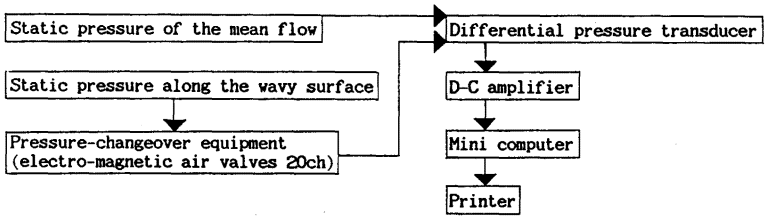

Figure 3 The total system for the measurement of the pressure distribution.

of the pressure transducer was connected to the static hole of a Pitot tube installed in 20 cm above the wavy surface.

The pressure distribution along the wavy surface was measured relative to the static pressure in the free stream by means of differential pressure transducer (P90DL) which has sensitivity 7 mm AqFS. The static pressure in the free stream was measured by using a Pitot tube, which was 20 cm above the wavy surface, where the effect of the wave surface on the static pressure was negligible. The Pitot tube was moved successively above each pressure hole.

The pressure-changeover equipment is composed of twenty electro-magnetic valves (TAIYO, MI210MO4C, SP310-MI), which can change the connection between the pressure holes and the pressure transducer successively and remotely.

Output signal from the differential pressure transducer was amplified with D-C amplifire and sent to the mini-computer (TEAC PS9000 MODEL216). The signal was sampled with sampling freqency of 100 Hz, and the time average of the data with 20 sec duration was taken.

Wind speeds used in the experiment are as follows;
$U_0 = 3.10, 4.15, 6.28, 8.03, 10.33$ (m/s) (for the sinusoidal wave)
$U_0 = 2.98, 3.91, 5.91, 8.03, 10.02$ (m/s) (for the Stokes wave)
The wind velocity U_0 is the maximum wind velocity over the wave surface, which has been determined from the wind profile.

Figure 3 shows the total system for the measurment of the pressure distribution.

3. Analysis of the pressure data

Fourier components and their phase angles relative to the wave surface were determined from the measured pressure distributions along the wavy surfaces through the FFT method, and the spatial change of the static pressure $P(x)$ was approximated by

$$P(x) = \sum_{i=1}^{4} A_{pi} \cos(k_i x - \theta_i),$$

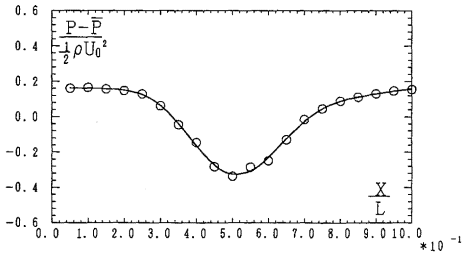

Figure 4 An example of the pressure profile along the Stokes wave: the solid curve represents the Fourier composition of four terms.

where A_{pi}, k_i and θ_i are the pressure amplitude, wave number and the phase of the i-th component respectively.

Figure 4 shows an example of the pressure profile along the Stokes wave. The solid curve shows the pressure profile obtained from above calculation. As shown in this figure, Fourier composition of four terms represents the measured pressure profile very well.

The pressure drag coefficient Cd is calculated from the measured pressure profiles $P(x)$ and surface profiles $\eta(x)$ by

$$\begin{aligned} Cd &= \frac{1}{L}\int_0^L P\cdot\frac{\partial\eta}{\partial x}dx \Big/ \frac{1}{2}\rho U_0^2 \\ &= \sum_{i=1}^{4}\frac{(ak)i}{2}\cdot Cp_i\cdot(-\sin\theta_i) \qquad \left(Cp_i = \frac{Ap_i}{\frac{1}{2}\rho U_0^2}\right) \\ &= \sum_{i=1}^{4} Cd_i \end{aligned} \tag{1}$$

where Cd_i, Cp_i and θ_i are called respectively as the pressure drag coefficient of wavy surface, amplitude coefficients and phase angle of pressure profile for each Fourier component.

The values of Cd, Cd_1, Cp_1 and $-\sin\theta_1$ of the pressure profiles measured along two wavy surfaces for various wind speeds are summarized in Table 2, where the wave steepness $(ak)_1$ and the Reynolds number defined as HU_0/ν are included, where H is the wave height, U_0 the maximum wind speed over the wavy surface and ν the coefficient of kinematic viscosity of the air. These data are used to investigate the relation between the pressure drag coefficient Cd and its control parameters such as the wave steepness ak or the Reynolds number HU_0/ν. In addition to the present data, we will also use the previous data obtained by other authors (Motzfeld[1], Kendall[2], Zilker et al[3][4] and Buckles et al[5]), which are summarized in Table 3.

Table 2 The value of Cd, Cd_1, Cp_1 and $-\sin\theta_1$ measured along the wavy surfaces for various Reynolds numbers $R_H = HU_0/\nu$.

Run. No.	*Wave*	$(ak)_1$	R_H	Cd ($\times 10^{-3}$)	Cd_1 ($\times 10^{-3}$)	Cp_1	$-sin(\theta_1)$
1	sine	0.314	4363	6.095	6.095	0.154	0.252
2	sine	0.314	5740	5,556	5.556	0.180	0.196
3	sine	0.314	8876	3.839	3.839	0.203	0.121
4	sine	0.314	10559	3.695	4.695	0.227	0.104
5	sine	0.314	13773	3.319	3.319	0.255	0.830
6	Stokes	0.308	3379	8.939	8.956	0.137	0.425
7	Stokes	0.308	5165	8.096	7.945	0.155	0.333
8	Stokes	0.308	7761	7.299	7.004	0.194	0.235
9	Stokes	0.308	10463	6.617	6.241	0.223	0.182
10	Stokes	0.308	12509	5.165	4.925	0.225	0.142

Table 3 The form parameters of the test waves used in the present study, Motzfeld, Kendall, Zilker et al and Buckles et al: R_L shows the Reynolds number based on the wave length.

Model	*Wave*	H/L	$(ak)_1$	$(ak)_2$	$(ak)_3$	$(ak)_4$	$R_L(\times 10^4)$
Present I	sine	0.1	0.314	0	0	0	4.0−14.0
Present II	Stokes	0.1	0.308	0.0779	0.0179	0.0053	2.0−13.0
Motzfeld I	sine	0.05	0.157	0	0	0	33.0
Motzfeld II	sine	0.1	0.314	0	0	0	33.0
Motzfeld III	trochoid	0.097	−	−	−	−	16.5
Kendall	sine	0.0625	0.196	0	0	0	1.9−6.4
Zilker I	sine	0.0125	0.039	0	0	0	1.1−6.4
Zilker II	sine	0.0312	0.098	0	0	0	
Zilker III	sine	0.05	0.157	0	0	0	
Zilker IV	sine	0.125	0.393	0	0	0	
Zilker V	sine	0.2	0.628	0	0	0	
Buckles	sine	0.2	0.628	0	0	0	1.2

4. Result

4.1 Pressure profile

Figure 5 shows the change of the static pressure profiles with the Reynolds number HU_0/ν. Ordinate is the pressure deviation from the mean static pressure over one wave length, which is normarized by $\frac{1}{2}\rho U_0^2$. Abscisa is the horizontal

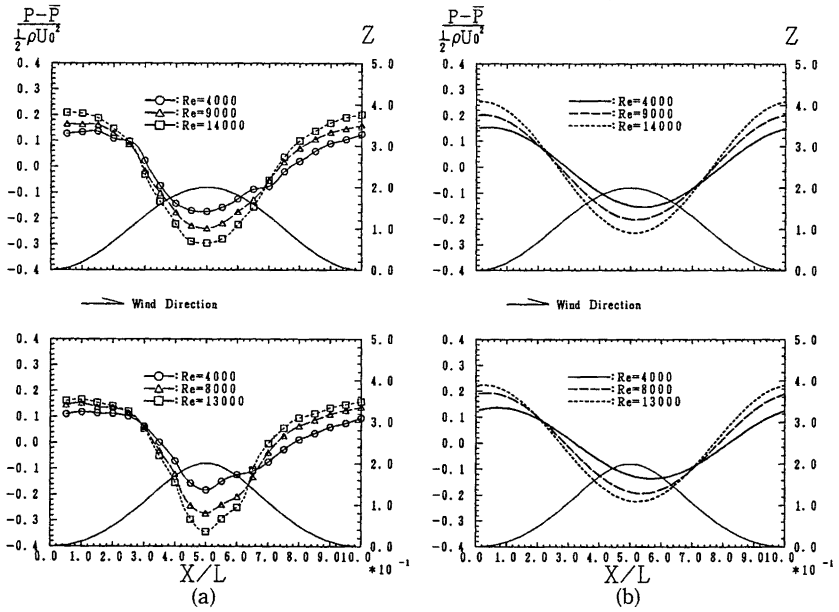

Figure 5 The change of the static pressure profile with the Reynolds number HU_0/ν : (a), measured profiles; (b), the first mode obtained from measured pressure profiles; the upper part shows pressure profiles along the sinusoidal wave and the lower part shows those along the Stokes wave; Bottom curve in each figure shows configuration of the wavy surfaces.

distance from the wind ward trough, which is normarized by the wave length L. The left hand side of this figure shows the pressure profiles measured along the sinusoidal wave and the Stokes wave. The right hand side shows those obtained from the first mode of each measured pressure profile. Figure 5 shows that amplitude of the normarized pressure profile increases with the increase of the Reynolds number, while its phase angle decreases with the increase of the Reynolds number.

Figure 6 shows the comparison of the first mode of pressure profile for the sinusoidal wave with that for the Stokes wave.

It can be seen from the data for $Re \fallingdotseq 4000$ that the phase of the first mode of the pressure profile for the Stokes wave is larger than that for the sinusoidal wave, while their amplitude is not much different. With the increase of the Reynolds number, the difference in the phase angle of the pressure profiles for two waves decreases gradually.

The results shown in Figs. 5 and 6 suggest the dependence of the pressure profiles along the wavy surface on the shape of waves and the Reynolds number, We will investigate their relations more quantitatively in the next section.

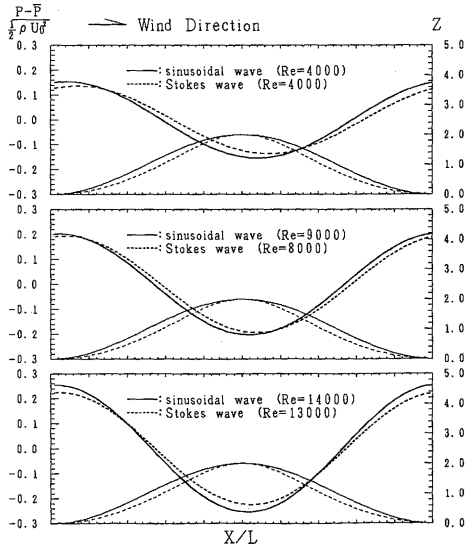

Figure 6 The first mode of measured pressure profiles along the sinusoidal wave and the Stokes wave: ——, the profile along the sinusoidal wave; ------, the profile along the Stokes wave; ——, configuration of the sinusoidal wave; -------, configuration of the Stokes wave.

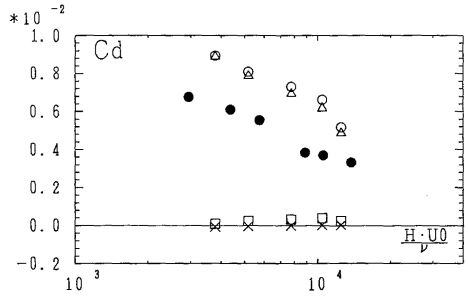

Figure 7 The pressure drag coefficients corresponding to the harmonic modes of the Stokes wave and those for the sinusoidal wave versus the Reynolds number HU_0/ν: ○, the total pressure drag coefficient Cd for the Stokes wave; △, first mode component Cd_1 for the Stokes wave; □, second mode component Cd_2 for the Stokes wave; ×, third mode component Cd_3 for the Stokes wave; ●, the total pressure drag coefficient Cd for the sinusoidal wave. (Note: $Cd_2 = Cd_3 = 0$ for the sinusoidal wave.)

4.2 Pressure drag coefficient

Figure 7 shows the pressure drag coefficients corresponding to the harmonic modes for the Stokes wave and those for the sinusoidal wave versus the Reynolds number HU_0/ν. It should be noted that the total pressure drag coefficient for the sinusoidal wave is equal to the pressure drag coefficient of the

first mode, because the higher harmonic modes of wavy surface is zero (see Eq. 1).

Even for the Stokes wave which contains higher modes, the total pressure drag coefficient for the Stokes wave is nealy equal to the pressure drag coefficient of the first mode. The ratio of the sum of the pressure drag coefficients due to the higher harmonic modes to the total pressure drag coefficient is less than 5% in the present range of the Reynolds numbers 4,000 ~14,000. Therefore, the total pressure drag coefficient is determined approxi-

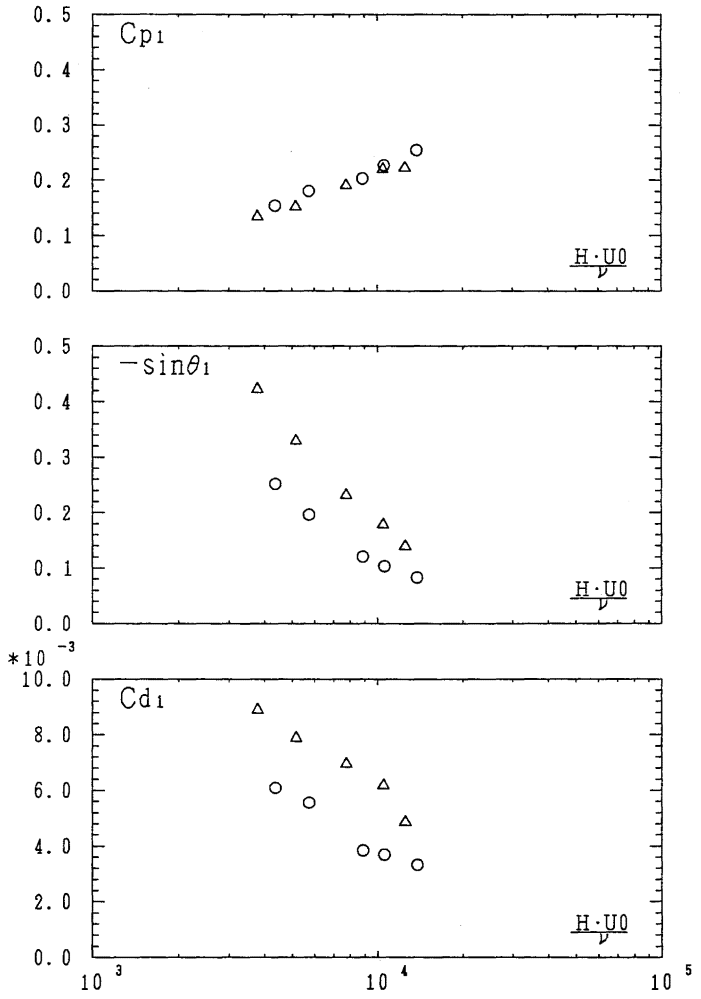

Figure 8 Cp_1, $-\sin\theta_1$ and Cd for the Stokes wave and for the sinusoidal wave versus HU_0/ν : ○, the properties for the sinusoidal wave ; △, the properties for the Stokes wave.

mately from the first mode quantities, the steepness $(ak)_1$, phase angle θ_1 and the amplitude coefficient Cp_1. by using Eq. (1).

As shown in Fig. 7, the pressure drag coefficient for the Stokes wave is larger than that of the sinusoidal wave. This fact is explained as follows. Figure 8 shows the comparisons of the amplitude coefficient Cp_1, phase angle θ_1 and the total pressure dag coefficient Cd for the Stokes wave with those of the sinusoidal wave.

The amplitude coefficient Cp_1 for the Stokes wave is almost the same to that for the sinusoidal wave in the range of the Reynolds number 4,000~14,000, and both of them decrease slowly with the increase of the Reynolds number.

On the other hand, the value of $-\sin\theta_1$ for the Stokes wave is larger than that for the sinusoidal wave, especially for the low Reynolds number, though the former decreases with the increase of the Reynolds number more rapidly than the latter and the former becomes nealy equal to the latter at $Re \fallingdotseq 20{,}000$.

From the results shown above, the following conclusion may be drawn ; the existence of the higher harmonic mode in the wavy surface such as in the Stokes wave increases the pressure drag coefficient of the wavy surface, and they are attributed mainly to the increase of the phase shift θ_1.

4.3 Parameterization of the pressure drag coefficient

The pressure drag coefficient of the solid wavy surface, Cd is considered as a function given by

$$Cd = F((ak)_i, Re_i, Re_2) \ , \qquad (i = 1, 2, 3, 4), \qquad (2)$$

where $(ak)_i$ is the wave steepness for each Fourier component of the wavy surface, Re_1 the Reynolds number based on the form parameter of the wavy surface, for example HU_0/ν, and Re_2 the Reynolds number based on the rough-

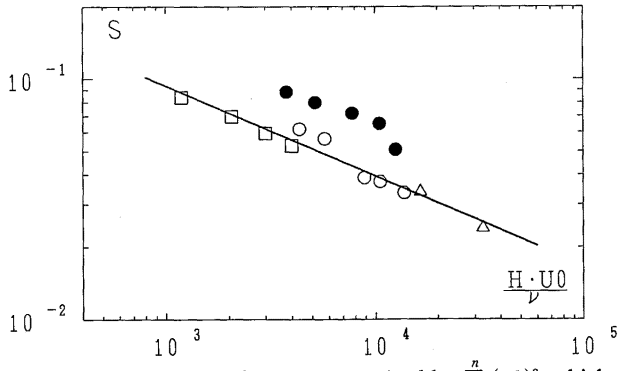

Figure 9 The pressure drag coefficients normarized by $\sum_{i=1}^{n}(ak)_i^2$, which are called as the sheltering coefficient $S(= Cd/\sum_{i=1}^{n}(ak)_i^2)$ versus the Reynolds number HU_0/ν : ○, present data for the sinusoidal wave ; ●, present data for the Stokes wave ; △, data for Motzfeld I, II ; □, data of Kendall.

ness parameter of the wave surface itself such as dU_0/ν (d ; roughness height along the wave surface).

In the present experiment, Re_2 is neglected because both wave surfaces are smooth. Therefore the pressure drag coefficient Cd is considered as function of $(ak)_i (i = 1, 2, 3, 4)$ and Re_1.

First we investigate the relation between the Reynolds number HU_0/ν and the pressure drag coefficient normarized by the value of $\sum_{i=1}^{n} (ak)_i^2$, which is called as the sheltering coefficient $S(= Cd/\sum_{i=1}^{n} (ak)_i^2)$ proposed by Jeffreys[6)7)].

Figure 9 shows this relation where the data of Mozfeld[1)] and Kendall[2)] are also included. The data reporeted by Zilker et al[3)4)] and Buckles et al[5)] is not included in this figure because they used, as a reference wind velocity, bulk velocity which is determined from the velocity profiles measured at the centre of the chennel when the wave section is replaced by a flat section. The solid symbol in this figure is the sheltering coefficient of the Stokes wave $Cd/\sum_{i=1}^{4} (ak)_i^2$. The sheltering coefficient for the sinusoidal waves $Cd/(ak)^2$ shows a unique dependence on the Reynolds number HU_0/ν and the relation is approximated by

$$\frac{Cd}{(ak)^2} = 1.230 \times \left(\frac{H \cdot U_0}{\nu}\right)^{-0.373} \tag{3}$$

However, the sheltering coefficient for the Stokes wave shows slightly defferent properties, which suggest the introduction of the other parameters.

Since the separation of the fluid from the wavy surface is considered to be controlled partly by the local slope of the wave surface, we introduce the

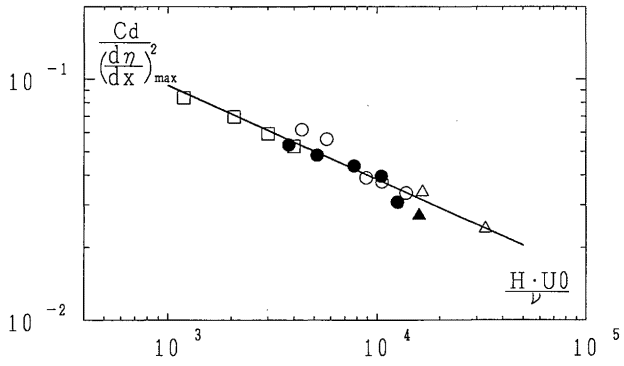

Figure 10 The pressure drag coefficients normarized by the square of the maximum slope $Cd/\left\{\left(\frac{\partial \eta}{\partial x}\right)_{max}\right\}^2$ versus the Reynold number $Re = HU_0/\nu$: ○, present data for the sinusoidal wave ; ●, present data for the Stokes wave ; △, data for Motzfeld I, II ; ▲, data for Motzfeld III ; □, data of Kendall.

maximum slope of the wave surface $\left(\frac{\partial \eta}{\partial x}\right)_{\max}$ as a controll parameter for the pressure drag coefficient. The maximum slope of the Stokes wave is given by

$$\left(\frac{\partial \eta}{\partial x}\right)_{\max} = \sum_{i=1}^{n} (ak)_i$$

Figure 10 shows the total pressure drag coefficient normarized by the square of the maximam slope $\left(\frac{\partial \eta}{\partial x}\right)^2_{\max}$ versus Reynolds number HU_0/ν. It is very interesting that the total pressure drag coefficients normaraized by the maximum slope of the various wavy surfaces, including the data of the Stokes wave and even for the trochoidal wave used by Motzfeld[1] is uniquly dependent on the Reynolds number HU_0/ν.

The relation determined by the least square method is given by

$$\frac{Cd}{\left\{\left(\frac{\partial \eta}{\partial x}\right)_{\max}\right\}^2} = 1.398 \cdot \left(\frac{H \cdot U_0}{\nu}\right)^{-0.391} \tag{4}$$

which is shown in Figure 10 with a solid line.

However, it should be noted that the wave with higher harmonics, which have been used in the present experiment, is confined only to the Stokes waves where the phases of the higher harmonics are fixed. Therefore, the further studies will be needed to generalize the present result, which include the studies on the pressure distributions on such waves as aymmetric waves and long waves covered by short waves.

5. Conclusion

Wind-induced pressure distributions along solid wavy surfaces have been investigated for two kinds of waves; the sinusoidal wave and the Stokes wave. The following conclusions can be drawn from the present study;

(i) The total pressure drag coefficient due to the air flow over the wavy surface can be approximated by the first mode of the drag coefficient which is calculated by the first mode of the pressure profile along the wavy surface even for the Stokes waves containing higher harmonics.

(ii) The amplitude coefficient of the first mode of the pressure distribution for the Stokes wave is nearly equal to that for the sinusoidal waves in the range of Reynolds numbers 4,000~14,000, while the phase shift of the first mode for the former is larger than that for the latter. Therefore, the total pressure drag coefficient for the Stokes wave is larger than that for the sinusoidal wave. That is, the existence of the higher harmonic modes in the wavy surface such as in the Stokes wave increases the pressure drag coefficient of the wavy surface and they are attributed to the increase of the phase shift θ_1.

(iii) The pressure drag coefficient normarized by the value of $\sum_{i=1}^{n} (ak)_i^2$, that is

called sheltering coefficient, is dependent on the Reynolds number HU_0/ν. The sheltering coefficients for the sinusoidal waves $Cd/(ak)^2$ show a unique dependence on the Reynolds number HU_0/ν. This relation is approximated by

$$\frac{Cd}{(ak)^2} = 1.230 \cdot \left(\frac{H \cdot U_0}{\nu}\right)^{-0.373}$$

However the sheltering coefficients for the Stokes waves $Cd/\sum_{i=1}^{4}(ak)_i^2$, is slightly larger than that for the sinusoidal wave at the same Reynolds number.

(iv) Then maximum slope of the wave surface $\left(\frac{\partial \eta}{\partial x}\right)_{\max}$ is introduced as a controll parameter for the pressure drag coefficient. The total pressure drag coefficient normarized by the square of the maximum slope $\left\{\left(\frac{\partial \eta}{\partial x}\right)_{\max}\right\}^2$ of the various wave surfaces is uniquly dependent on the Reynolds number HU_0/ν. This relation is given by

$$\frac{Cd}{\left\{\left(\frac{\partial \eta}{\partial x}\right)_{\max}\right\}^2} = 1.398 \cdot \left(\frac{H \cdot U_0}{\nu}\right)^{-0.391}$$

Acknowledgment

The authors wish to express their gratitudes to Dr. A. Masuda for his helpful discussions. This study was suported by the Grant-in-Aide for Scientific Reserch, Project B No. 60460049 from the Ministry of Education Science and Culture of Japan.

References

1) Motzfeld, H.: Die turbulente Strömung an welligen Wänden. Z. Angrew. Math. Mech., Vol. 17, (1937) 193-212.
2) Kendall, J. M: The turbulent boundary layer over a wall with progressive surface waves. J. Fluid. Mech. 41, (1970) 259-281.
3) Zilker, D. P., Cook, G. W, and Hanratty, T. J: Influence of the amplitude of a solid wavy wall on a turblent flow. Part 1. Non-separated flows. J. Fluid. Mech. 82, (1977) 29-51.
4) Zilker, D. P. and Hanratty, T. J: Influence of the amplitude of a solid wavy wall on a turblent flow. Part 2. Separated flows. J. Fluid. Mech. 90, (1979) 257-271.
5) Buckles, J., Hanratty, T. J and Adrian, R. J.: Turbulent flow over large-amplitude wavy surfaces. J. Fluid. Mech. 140, (1984) 27-44.
6) Jeffreys, H.: On the formation of waves by wind. Proc. Roy. Soc., Vol. 107, (1924) 189-205.
7) Jeffreys, H.: On the formation of waves by wind II. Proc. Roy. Soc., Vol. 110, (1925) 241-247.

(Received December 21, 1987)